

Numerical Prediction of the Effect of Cyclonic Wind Pressures on the Solar Panels

Yash Deepak Chadha¹, Sunny Kumar Barnwal²

¹Jamnabai Narsee International School, Mumbai, India.

²Indian Institute of Technology Bombay, Mumbai, India.

Abstract – A commercial solar panel of standard dimensions is simulated in Abaqus™ for different pressure loads for the respective five cyclonic wind speed categories viz., 120, 150, 180, 210 and 250 kmph. The model was implemented with five sub-layers inside the thin solar panel to understand the stress response at every layer corresponding to glass, encapsulation, cell and back-sheet. A 5mm thick panel was investigated with solar cell having a standard 0.5mm thickness. The drag and lift coefficients for different wind speeds over a flat plate at 25° inclination were obtained from the existing literature and the pressure force components were analytically calculated. These forces were resolved into the normal and parallel directions to the panel surface. The force in the direction surface traction force i.e., the shear force over the top surface panel was found to be significantly higher than the force normal to the panel. This behaviour hinted at the tendency of solar panel to strain more in the upward direction, parallel to the top surface. This is due to the increase of lift coefficient with increase in wind speed.

Key Words: Solar panel stress, cyclone wind effect, panel drag and lift, multilayer panel analysis

1. INTRODUCTION

High wind speeds pose significant challenges to the structural integrity of solar panels. The force exerted by strong winds can lead to mechanical stress on the panels and their mounting systems. This stress may result in physical damage, such as cracks or breaks in the panels or their frames. In extreme cases, it can even cause the panels to detach from their mounts. Additionally, wind-induced vibrations can accelerate wear and tear on the panel components over time. To address these issues, solar panel installations in areas prone to high winds require robust mounting systems, regular inspections, and proper maintenance to ensure the longevity and reliability of the solar energy system.

There have been a few attempts at this problem as observed from the literature. Sauca et al. compared wind load calculations using numerical simulation (CFD) and manual calculations based on design codes. Manual calculations overestimated forces due to not considering panel arrays, with differences of around 31% for drag force and over 10% for lift force compared to CFD results. While, Shademan et al. examine force distribution on standalone and arrayed solar

panels under various wind conditions and inclinations, revealing key design considerations such as the critical gap spacing for minimizing drag. However, a comprehensive study of wind loading on different layers of the photovoltaic module is lacking.

In order to understand the stress response across the assembled solar panel, embedded in an aluminium frame, every layer inside the solar panel consisting of glass encapsulant (EVA) photovoltaic cell (silicon wafers) and the back-sheet (tedlar) was numerically assembled and simulated for different wind pressures. The high-speed winds of 120, 150, 180, 210 and 250 kmph were considered to evaluate the impact on the thin solar panel. This range of velocity has been categorized into five cyclone categories by the National Disaster Management Authority, Govt. of India, with wind speed of 250 or above kmph is considered as catastrophic cyclone of category 5.

The importance of this study lies in the stress response analysis of the very thin individual sub-layers in the solar panel to the five cyclonic winds. This analysis can help designing the reinforcements to the solar panel and its supports in the cases of such natural disaster.

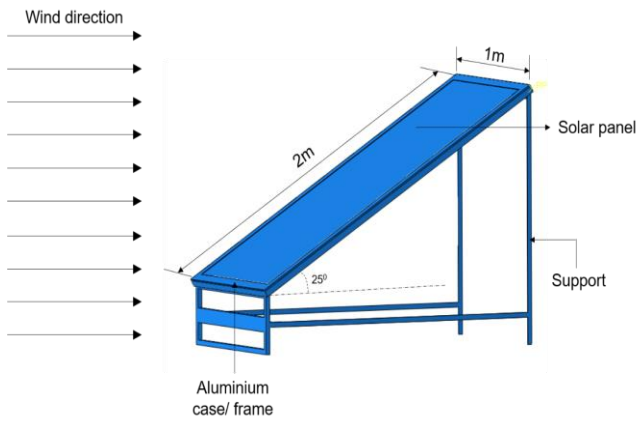
Table 1: Cyclone wind speeds categories as per National Disaster Management Authority, Govt. of India

Cyclone category	Wind speeds (km/hr)	Damage Capacity
1	120-150	Minimal
2	150-180	Moderate
3	180-210	Extensive
4	210-250	Extreme
5	250 and above	Catastrophic

2. MATHEMATICAL MODEL

A dynamic explicit finite element (FE) model was implemented in Abaqus™ with the solar panel meshed with hex element C3D8R i.e., 3-dimensional cubic element with reduced integration points. The solar panel was embedded in aluminium frame and the frame was assembled on the steel support as shown in figure 1(a). The solar panel was

provided the dimension of 2m x 1m and a 5mm thickness (figure 1(b)). The thickness of each layer obtained from Li, 2020 is given in table 1 given. The materials are assembled in the panel in an order as mentioned serially in table 2. The solar cell is sandwiched between the encapsulant, EVA.



(a)



(b)

Figure 1: (a) Assembly of solar panel in a case, inclined at 25° on a fixed support and; (b) Sub-layers inside the 5mm thick solar panel. Each layer was provided respective material property for the finite element analysis.

Table 2: Thickness and properties of materials used in the solar panel.

Sr. no.	Material	Thickness (mm)	Density (Kg/m ³)	Young's modulus (Pa)
1	Glass	3.2	3000	70 e+09
2	EVA	0.5	960	65 e+06
3	Cell	0.5	2330	168 e+09
4	EVA	0.5	960	65 e+06
5	Tedlar	0.3	1200	3.5 e+09

2.1 Wind speeds and corresponding wind pressures

Solar panels are usually inclined at 25° with the horizontal. The pressures exerted by the winds were calculated for each of the five cyclonic winds. The forces exerted are the drag (skin friction and wake), lift and wind impact. Skin friction was calculated and found to be significantly less in comparison to the wake drag, hence it was neglected in the actual FE analysis.

The coefficients of drag (C_D) and lift (C_L) for winds flowing over a flat surface at this inclination were referred from the studies of Ortiz et al., 2015 and Pieris et al., 2022. The C_D and C_L were assumed constant for the current analysis for all the speeds owing to lower fluctuations of both the coefficients at the given angle of attack. The pressures applied due to drag and lift are given below in equations (1) and (2).

$$P_{drag} = \frac{1}{2} C_D \rho U_{\infty}^2 \quad (1)$$

$$P_{Lift} = \frac{1}{2} C_L \rho U_{\infty}^2 \quad (2)$$

Here P is the pressure due to drag or lift. ρ is the air density and U_{∞} is the free stream velocity. The wind speeds are in the turbulent regime and the coefficients are directly used from the literature which have considered the turbulent effects while identifying the coefficients. Hence, these coefficients are directly used to calculate the pressures exerted to perform stress analysis.

Later, the impact of the wind flowing at velocity v due to its momentum was found as below by using Newton's second law of motion. Here, F is force and m is mass.

$$F_{impact} = \frac{d}{dt} (mv) \quad (3)$$

$$F_{impact} = \frac{dm}{dt} v + m \frac{dv}{dt} = \dot{m}v + m\dot{v} \quad (4)$$

But considering the current case where the velocity is to be considered constant for the impact calculation, the term $m\dot{v}$ becomes zero as there is no change in velocity. Hence, the equation 4 becomes,

$$F_{impact} = \dot{m}v \quad (5)$$

$$F_{impact} = \rho \dot{V}v \quad (6)$$

\dot{V} is the rate of change of volume.

$$F_{impact} = \rho(Av)v \quad (7)$$

$$F_{impact} = \rho Av^2$$

$$P_{impact} = \rho v^2 \tag{8}$$

i.e.;

$$P_{impact} = \rho U_{\infty}^2 \tag{9}$$

Equation (9) was used to calculate pressure due to wind impact.

2.2 Boundary Conditions

The steel support was provided with a fixed boundary condition (all displacements as zero). All the three pressure forces were resolved and applied in two directions viz., along the panel which is also called as surface traction and normal to the panel as shown in figure 2. The pressures due to lift and wind impact were applied on the top surface of the panel, which has glass material on its side. The drag force is mainly due to wake, hence it was applied at the back side of the panel, where the back-sheet material was present.

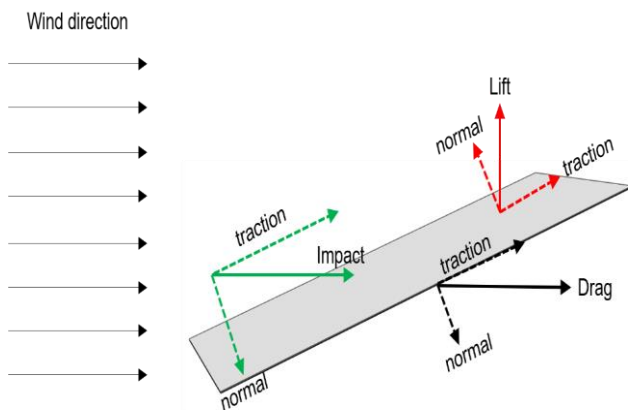


Figure 2: Schematic of resolution of wind pressure forces along and normal to the panel

3. RESULTS AND DISCUSSION

The wind pressures for the five speeds were calculated based on the equations (1), (2) and (9). The wind impact had the highest magnitude among the three forces (which is also due to smaller C_D and C_L for this angle of attack). As can be seen in figure 2, all the forces along the panel i.e., the traction forces add up to form the strongest force component on the panel.

Figure 3 depicts von mises stress contours for the five cyclone categories. The category 5 owing to the highest wind speed has shown more stress concentration than the others. It can be observed that although the panel is acted upon by a uniform pressure force, there is straining gradient across the panel. This is specifically due to the contact of case and

support at the edges. These edges are hence prone to stress concentrations. It can also be noted that, the point of least stress is not at the center of the panel but slightly offset and downstream along the panel. This is due to the traction force was acting from bottom to top, hence, there is no symmetry in stress response about the mid-plane.

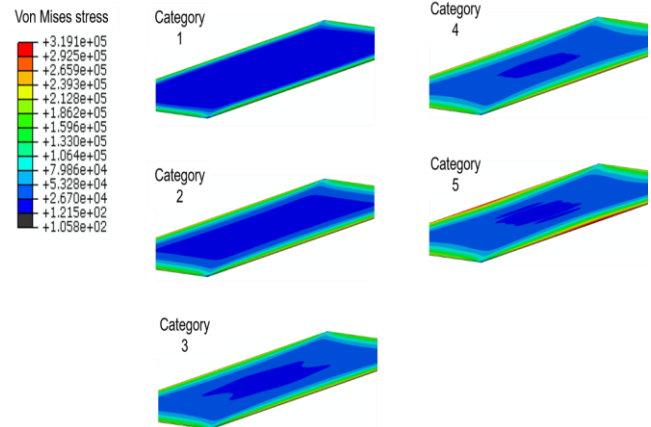


Figure 3: Cyclone category-wise von mises stress contour plots

The stress distribution at the edges was further explored to identify the variation across the panel thickness. Figure 4 shows the highest stress accumulation at the solar cell layer between the EVA encapsulants. The back-sheet and the encapsulants have significantly lesser stress. This behaviour is also due to the relatively highest Young's modulus of the solar cell material, increasing the elastic stress. The encapsulants, due to lower Young's modulus could strain more and absorb the pressure, which resulted into lower stress values.

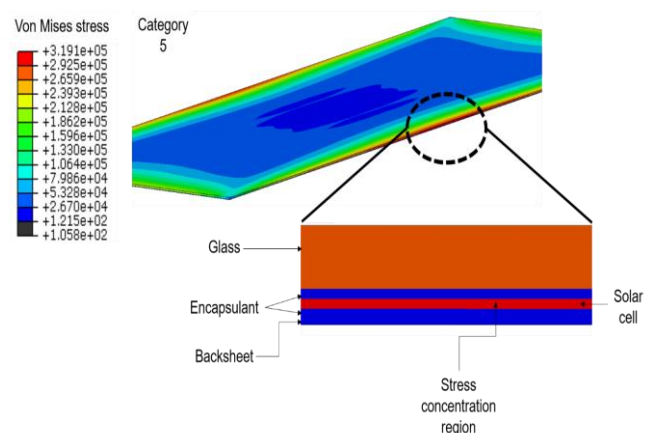


Figure 4: Variation in stress across the thickness of the panel. Stress concentration region at the solar cell.

Further, in order to understand the extent of difference of stresses between the middle and the edge regions in the panel, a point was selected on the mid-plane at the middle and at the edge, in the solar cell layer as shown in figure 5(a).

The stress responses across all the wind speeds at both the points were compared as in figures 5(b) and 5(c). The edge showed roughly ten times more stress concentration than the middle region, owing to the boundary condition in the form of the aluminium case as shown in figure 1(a). This simulation hence suggests an incorporation of such boundary condition to the panel while analyzing the stresses.

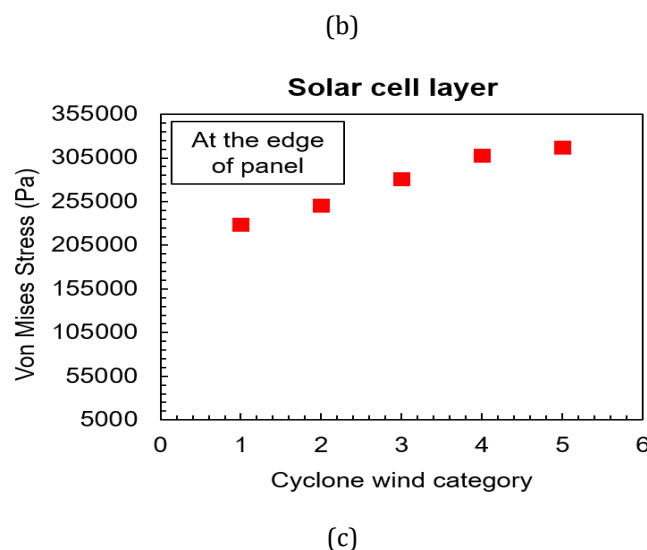
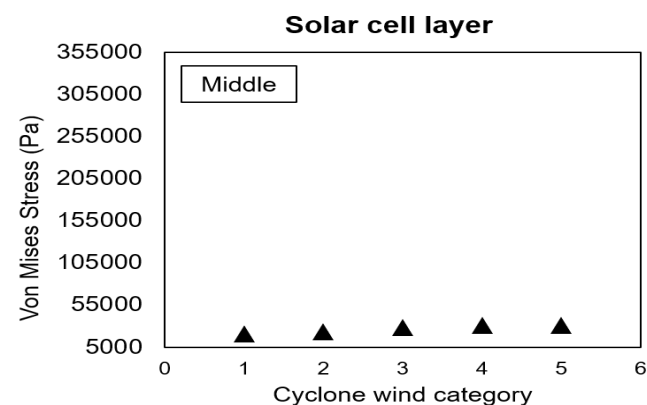
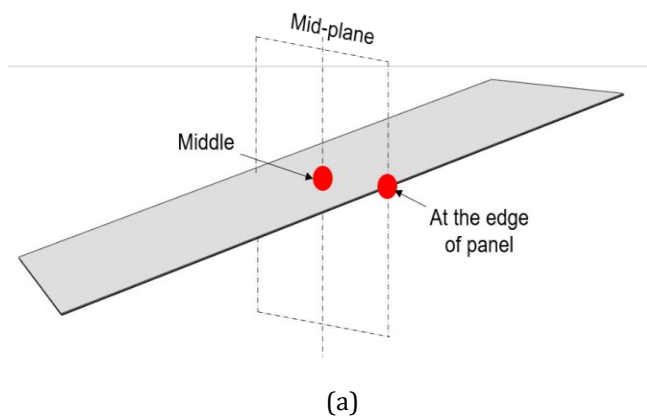


Figure 5: (a) Schematic of the points at which the simulated data is extracted for von mises stress at 5 wind

speeds; (b) Mises stress at the middle point in the mid-plane of the solar cell layer at different wind speed categories and; (c) Mises stress at the edge in the mid-plane of the solar cell layer at different wind speed categories

4. CONCLUSIONS

Finite element simulations were performed in Abaqus™ to predict the stress across the solar panel inclined at 25° against five different wind speed loads corresponding to five cyclone categories. The simulations consisted of a composite solar panel of 5 sub-layers having different material properties.

- The analytical calculations of wind pressures suggested a higher surface traction force on the panel than the force normal to it
- The simulations suggest a relatively high concentration region at the solar cell layer though the magnitude is lesser than the plastic range.
- The edge of the solar layer displayed significantly higher stress concentration than the middle portion, owing to the case fixture being attached at that location.
- This study can help in analyzing and designing the safety reinforcements for the solar cell layer in the solar panels, especially while designing at high wind speed prone areas.

REFERENCES

- [1] Abaqus Documentation, 2017.
- [2] Li, Z., 2020, September. Stress analysis of the solar cells in pv modules. In *Journal of Physics: Conference Series* (Vol. 1622, No. 1, p. 012123). IOP Publishing. doi:10.1088/1742-6596/1622/1/012123
- [3] Natural disaster management authority, Govt. of India. <https://ndma.gov.in/Natural-Hazards/Cyclone>
- [4] Ortiz, X., Rival, D. and Wood, D., 2015. Forces and moments on flat plates of small aspect ratio with application to PV wind loads and small wind turbine blades. *Energies*, 8(4), pp.2438-2453. <https://doi.org/10.3390/en8042438>
- [5] Pieris, S., Yarusevych, S. and Peterson, S.D., 2022. Flow development over inclined flat plates in ground effect and relation to aerodynamic loads. *Physics of Fluids*, 34(9). <https://doi.org/10.1063/5.0102406>

- [6] Sauca, A. C., Milchiş, T., & Gobesz, F. Z. (2019). Wind loading on solar panels. *Műszaki Tudományos Közlemények*, 10(1), 73-78.
- [7] Shademan, M., & Hangan, H. (2009, June). Wind loading on solar panels at different inclination angles. In *11th Americas conference on wind engineering* (pp. 22-26).